

DISCLAIMER

Copyright 2006 Society of Photo-Optical Instrumentation Engineers.

This paper will be published in SPIE conference Orlando May 2006 proceedings and is made available as an electronic preprint with permission of SPIE. One print or electronic copy may be made for personal use only. Systematic or multiple reproduction, distribution to multiple locations via electronic or other means, duplication of any material in this paper for a fee or for commercial purposes, or modification of the content of the paper are prohibited.

The OmegaCAM 16K x 16K CCD Detector System for the ESO VLT Survey Telescope (VST)

Olaf Iwert^a, D. Baade^a, A. Balestra^a, A. Baruffolo^b, A. Bortolussi^a, F. Christen^c, C. Cumani^a, S. Deiries^a, M. Downing^a, C. Geimer^a, G. Hess^a, J. Hess^d, K. Kuijken^e, J. Lizon^a, B. Muschiello^d, H. Nicklas^f, R. Reiss^a, J. Reyes^a, A. Silber^a, J. Thillerup^a, E. Valentijn^c

^a European Southern Observatory, Karl-Schwarzschild-Strasse 2, 85748 Garching, Germany

^b Osservatorio Astronomico Di Padova, Vicolo dell' Osservatorio 5, 35122 Padova, Italy

^c Kapteyn Institute, P.O. Box 800, 9700 AV Groningen, The Netherlands

^d Universitäts Sternwarte München, Scheinerstr. 1, 81679 München, Germany

^e Sterrewacht Leiden, PO Box 9513, 2300 RA Leiden, The Netherlands

^f Insitut für Astrophysik, Friedrich-Hund-Platz 1, 37077 Göttingen, Germany

ABSTRACT

A 16K x 16K, 1 degree x 1 degree field, detector system was developed by ESO for the OmegaCAM instrument for use on the purpose built ESO VLT Survey Telescope (VST). The focal plane consists of an 8 x 4 mosaic of 2K x 4K 15um pixel e2v CCDs and four 2K x 4K CCDs on the periphery for the opto-mechanical control of the telescope. The VST is a single instrument telescope. This placed stringent reliability requirements on the OmegaCAM detector system such as 10 years lifetime and maximum downtime of 1.5 %. Mounting at Cassegrain focus required a highly autonomous self-contained cooling system that could deliver 65 W of cooling power. Interface space for the detector head was severely limited by the way the instrument encloses the CCD cryostat. The detector system features several novel ideas tailored to meet these requirements and described in this paper:

Key design drivers of the detector head were the easily separable but precisely aligned connections to the optical field flattener on the top and the cooling system at the bottom. Material selection, surface treatment, specialized coatings and in-situ plasma cleaning were crucial to prevent contamination of the detectors. Inside the cryostat, cryogenic and electrical connections were disentangled to keep the configuration modular, integration friendly and the detectors in a safe condition during all mounting steps. A compact unit for logging up to 125 Pt100 temperature sensors and associated thermal control loops was developed (ESO's new housekeeping unit PULPO 2), together with several new modular Pt100 packaging and mounting concepts. The electrical grouping of CCDs based on process parameters and test results is explained. Three ESO standardized FIERA CCD controllers in different configurations are used. Their synchronization mechanism for read-out is discussed in connection with the CCD grouping scheme, the shutter, and the integrated guiding and image analysis facility with four independent 2K x 4K CCDs. An illustration of the data chain performance from CCD output to storage on hard-disk gives an impression of the challenge to shift 512 MB of data within 45 seconds via the standardized hierarchical ESO data acquisition network. Finally the safety and emergency features of the overall system are presented.

Key words: mosaic, multiple controllers, synchronization, contamination, plasma cleaning, straylight, coating, cooling, Pt100, safety

1. INTRODUCTION

A 16K x 16K detector system was developed for the OmegaCAM instrument at the newly constructed ESO VLT Survey Telescope (VST; Capaccioli et al. 2005), featuring a 1 degree x 1 degree field. While the OmegaCAM instrument was built by a multinational consortium (Kuijken et al. 2004), the 16K x 16K OmegaCAM Detector System was developed by ESO, but funded by the consortium. The focal plane consists of an 8 x 4 mosaic of 2K x 4K e2v CCDs with 15 μ m pixels, accompanied by four 2K x 4K CCDs on the periphery for the opto-mechanical control of the telescope.

2. THE OMEGACAM INSTRUMENT

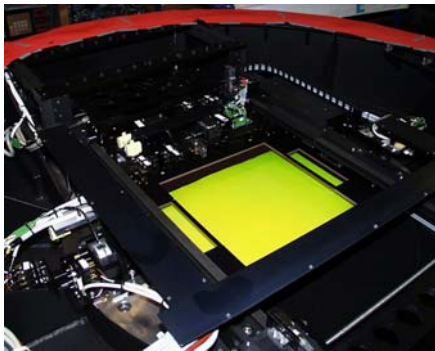


Figure 1: Filter in docking and locking mechanism

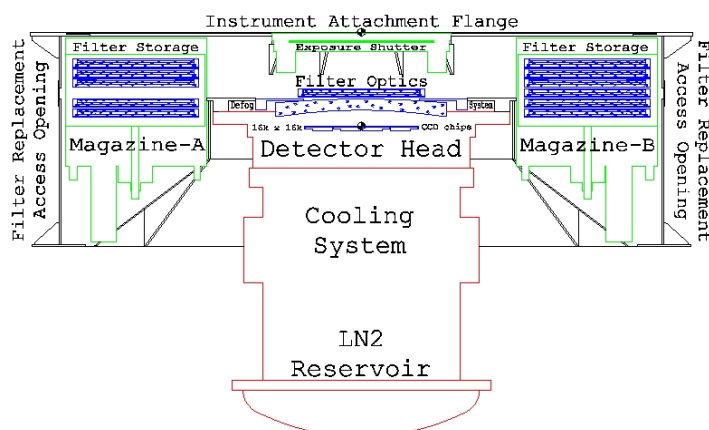


Figure 2: The OmegaCAM instrument (top view)

Figure 1 shows a filter in the optical beam directly on top of the focal plane. The dedicated filters of the auxiliary CCDs can clearly be seen. Figure 2 gives an overview of the OmegaCAM instrument from the topside which mounts to the VST Cassegrain interface flange. The filter shown in Figure 1 is initially inserted by means of the attached platform (mounted on the outside of the instrument) into one of the two filter magazines (top and bottom orientation in Figure 2). It is picked up, moved and locked stable in the beam by the docking and locking mechanism. The slit shutter designed by the University of Bonn is shown on top of the filter mechanism and operates with two moving Carbon blades bidirectionally to left and right side. Based on the optical design – but opposite to other instruments - all filter movements take place below the shutter. Therefore the light tightness of the instrument is vital for the detector operation, as a filter exchange typically occurs during the CCD detector readout of the previous image.

3. INTERFACES & MAIN REQUIREMENTS OF THE DETECTOR SYSTEM

Compared to the ESO 8K x 8K Wide Field Imager (Iwert 1998, unpublished) the 16K x 16K OmegaCAM detector system is not just a fourfold replica. In the OmegaCAM case the basically identical 2K x 4K unit detectors have to be butted on four sides. This leads to considerable complexity of the mechanics and electronics within the cryostat head. In spite of this, the two instruments and telescopes have comparable size, so that the overall filling factor at the Cassegrain focus is very much larger, and the instrument reaches the weight and torque limits of the VST.



The very small back-focal distance forces the cryostat to be deeply imbedded into the instrument while the optical design foresees - as an additional

flexrigid connector boards (Figures 6 & 8). All detectors have been tested and qualified individually on the ESO test bench against the contractual specifications. As the CCDs in each quadrant of the cryostat are partially sharing parallel and serial clocks, they have for each quadrant been selected according to their channel potential.

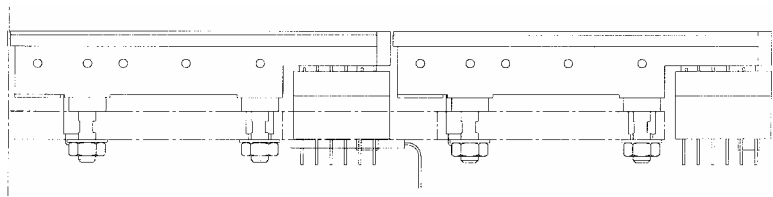


Figure 6: Cut view of 4 side butting with ZIF socket and flexrigid connector board (2004).

The cosmetic defects are well below the specified global defect budget. CCD flatness and accurate package metrology by e2v eased the integration into the mosaic without further spacer adaptations. More details about the individual testing procedures for these detectors can be found in Christen et al.

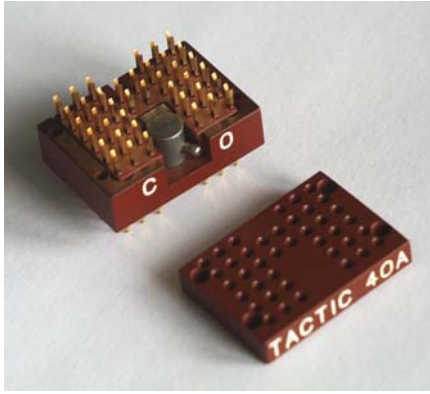


Figure 7: Custom made ZIF socket for four side buttability

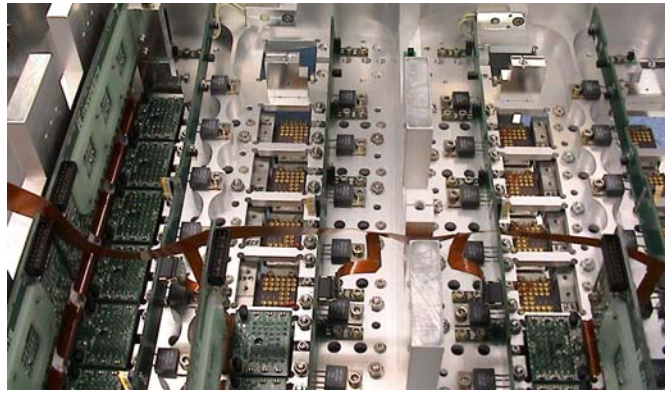


Figure 8: Photograph onto bottom of four side butting

5. THE DETECTOR HEAD

The cryostat head is the nexus of all interfaces of the detector system. Conflicting requirements from different domains had to be accommodated while the instrument was developed external to ESO. As the cryostat could not be prototyped due to cost and time, all solutions had to be designed in one go for the final product. The outside space limitations from the surrounding instrument together with the circular field flattener imposed a high filling factor and several form factors onto the cryostat. Following the symmetrical focal plane layout with 'left, left, right, right' CCD output register location (per mosaic row), the mechanics of the detector head was designed with a square housing. But the instrument housing (above) and the cooling system (below) are both circular. Symmetrical mechanical design - wherever possible - helped the modularity, the thermal properties of the CCD mosaic table, as well as the space, flexure and earthquake safety constraints.

Due to the limited access to all parts inside the cryostat and the fact that all mechanical and electronics parts had to be mounted without prior prototypes, the system was in a first step integrated without ultra-cleaning. After some small modifications the final cleaning was applied with strategies suitable to the types of materials in question. Owing to the sheer size of the parts conventional cleaning methods could not always be applied. Therefore - amongst others - plasma cleaning was employed in-situ in the cryostat vessel. (Further details can be found in Deiries et al. 2005.) Thereafter the clean cryostat head was integrated inside the clean room with the other cleaned component groups. Over some months, it was gradually put into cryogenic and electrical operation. The CCD mosaic was stepwise populated and tested with different numbers and different grades (mechanical, engineering, science) of detectors in order to reduce the possible impact of risks of mechanical, chemical, and electrical damage.

Key design drivers of the cryostat detector head were therefore symmetry, modularity, and easy access to all parts during all phases of assembly, integration, and testing.

On the outside this concerned mainly the easily separable but precisely tilt-aligned and centered optical field flattener with integrated defogging system at the top and the cooling system at the bottom with a special interface for the easy lift-off of the detector head (Figures 20 & 19).

Inside the detector head, cryogenic connections and electronic boards had to be disentangled such as to make them from the beginning independent and not crossing each other, so that each part inside the detector head can be integrated or disintegrated at any time without a need for removing others (Figures 9 & 10).

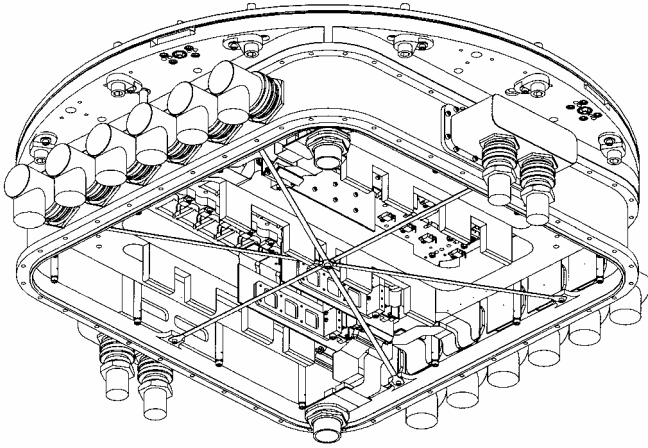


Figure 9: 3D bottom view of partially integrated CCD head

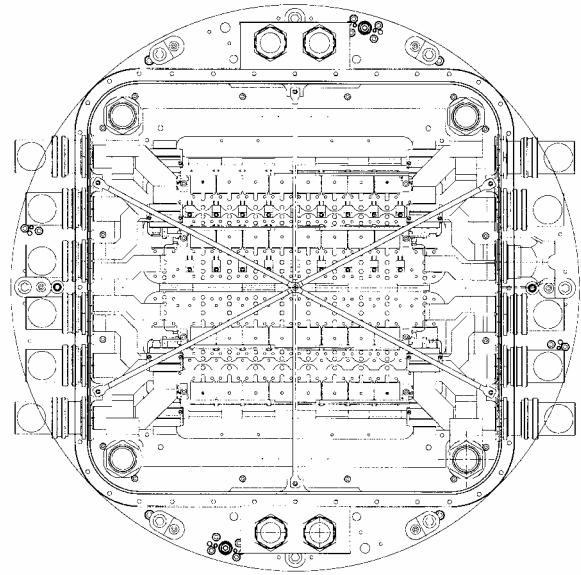


Figure 10: Bottom view of CCD head, fully symmetric design

In spite of the external diameter of 70 cm, the overall alignment error budget required all critical parts to be machined with a precision of a few microns.

In order to ensure the effective cooling of the CCD mosaic, all intermediate levels of cooling parts were largely abandoned. The CCD mosaic table was produced of aluminum based on previous experience and its ability to distribute thermal energy quickly and uniformly. Following detailed calculations, this base plate was designed as a light-weight but stiff 3D structure by integrating it into an outer frame. On the top side (Figure 11) it resembles a Swiss cheese for the mounting openings of CCDs and ZIF sockets, the bottom side (Figure 12) interfaces with its cold fingers directly to the clamps that connect it both mechanically and thermally to the cooling system. After application of different machining technologies and many thermal cycles to release mechanical stress, a flatness of some μm was achieved. It is held and thermally isolated by fiberglass parts which were dimensioned according to the flexure budget and earthquake safety. All fiberglass parts have been Parylene coated to reduce outgassing in the vacuum.

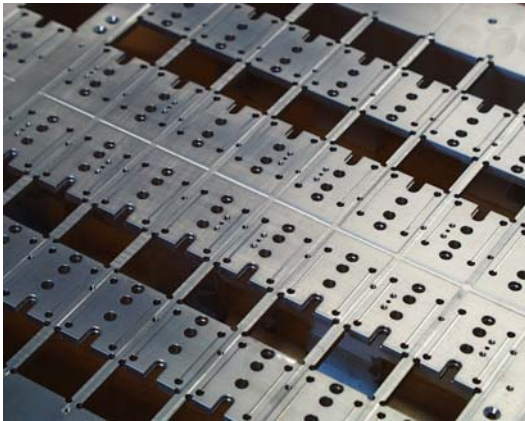


Figure 11: Detail top view of mosaic table

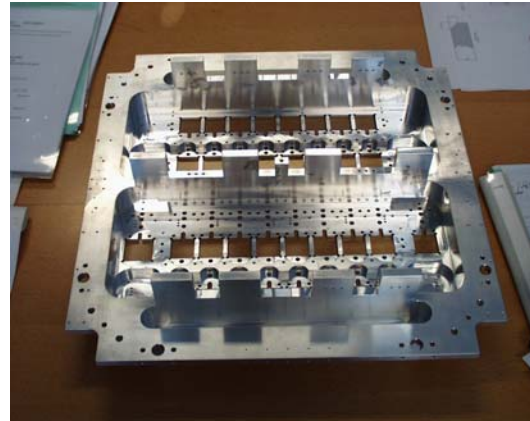


Figure 12: Bottom view of mosaic table

The integrated electronics with about 1400 contacts to the outside world was designed such as to have low thermal conductivity, high modularity, and good signal separation. As a trade-off between manufacturing cost and routing space a 'four-in-one bus board' was developed. It is mounted in the bottom cavities of the mosaic table. Per quadrant, two of these boards support eight CCDs and interface with one flexrigid interface board per signal group to a total of three

vacuum connectors with 128 pins each (Figure 13). The connections for each of the four auxiliary CCDs are fed through this board set of the respective nearest quadrant. The symmetry of the focal plane in connection with the symmetry of the mechanics permits the electronics of two quadrants each to be identical with the two pairs being mirror images of one another. All quadrants link to identical outside cabling for testability and ease of cabling. A total of 28 flexrigid boards have been designed and handrouted in complex 3D shapes for the cryostat system (Figure 14). The use of glue-free materials was mandatory to avoid contamination.

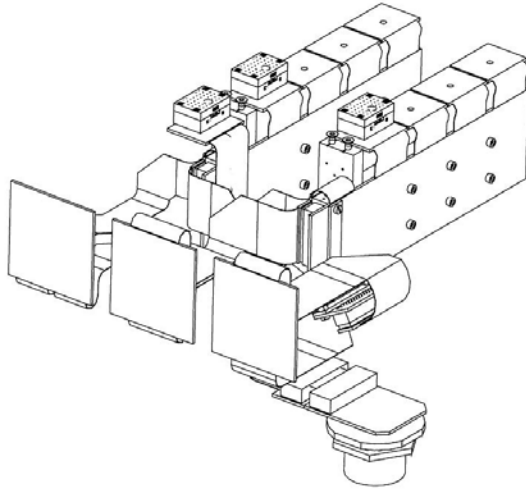


Figure 13. One quadrant of cryostat electronics

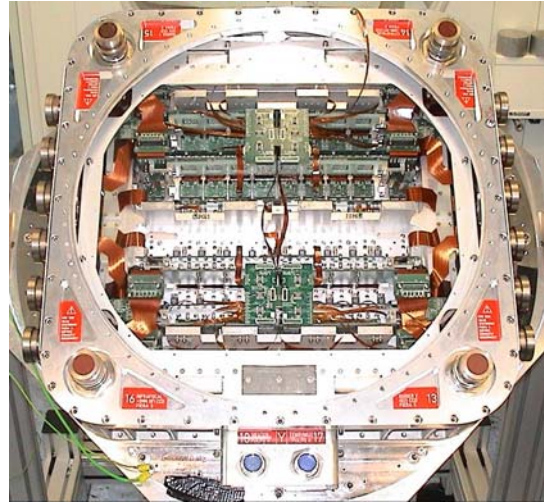


Figure 14. Bottom view of fully equipped open cryostat head

All parts and baffles in the light entrance part between auxiliary CCDs and CCD mosaic were blackened with Kepla coating to avoid contamination and straylight (Figure 15). An actively cooled shield acts as ice barrier. The shiny bond wires of the CCDs were masked with both cold and warm shields (Figure 16). After stepwise qualification of all alignment-critical parts, the CCD mosaic flatness was laser-triangulated at -120 C (and through a special dewar entrance window without optical power); a value of $40\text{ }\mu\text{m}$ (pp) had been achieved.

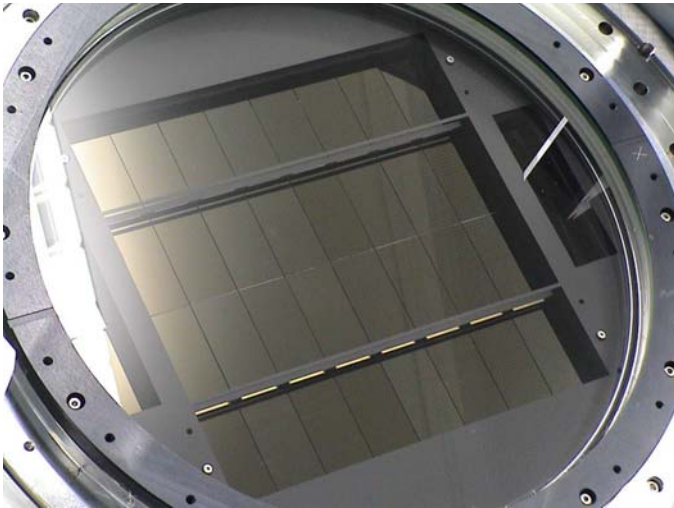


Figure 15: The 16K x 16K mosaic

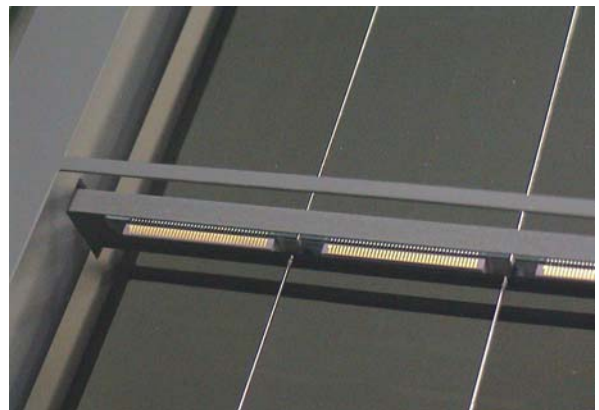


Figure 16: Close-up of bond wire baffling

6. THE COOLING SYSTEM

According to model calculations a heat load of 65 W had to be compensated by the cooling system, mounted below the CCD detector head. As no options for external compressors or the feeding of cooling lines through the telescope cable wrap existed, a self contained LN2-based system was developed. It utilizes the maximum cooling power of liquid nitrogen through the combination of an integrated 40 liter LN2 tank, combined with the main top heat exchanger operated in continuous flow mode by the cryostat cooling controller (Figure 16). The LN2 tank is internally fitted with an anti-overflow system, which allows to fill 85% of the volume independently of the telescope movement at Cassegrain focus. The continuous flow system cycles the nitrogen through the top heat exchanger and produces a position angle independent temperature distribution for the CCD mosaic plate. The top heat exchanger interfaces via a clamp system to the detector head (Figure 17).

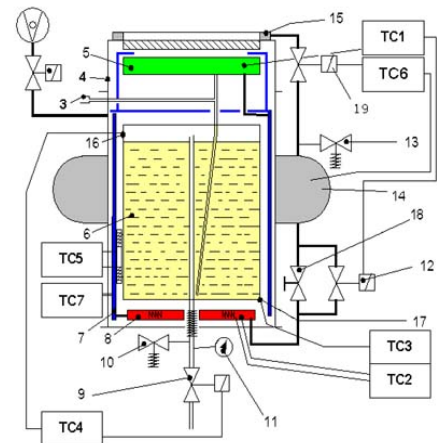
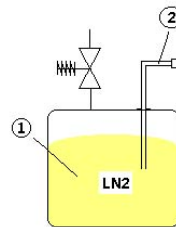
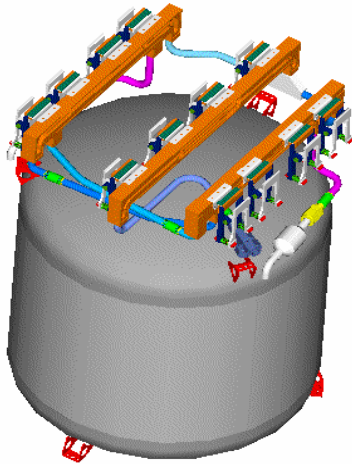


Figure 17: Internal LN2 tank and top heat exchanger with cold clamps

Figure 18: Operation scheme of cooling system

Figure 18 shows the cooling-system with all required components, including the external nitrogen storage tank used *only* for the refilling. In the following the interaction of the various cooling system components is explained :

In normal operation the storage tank (1) is not connected and the filling port is automatically closed by a spring loaded valve. This allows the pressure inside the internal tank (6) to build up to 0.6 bar.

The pressure is defined by the over pressure release valve (10) and can be verified at any time with the manometer (11). This over pressure forces the nitrogen out of the internal tank. A PID thermal controller (TC1) is used to keep the temperature of the top heat exchanger (5) to T1 such that T1 is a few Kelvin below the CCD operating temperature. TC1 opens the regulation valve (12) in order to lower T1. This leaves the nitrogen circulating inside the cooler. Leaving the cooler, the cold nitrogen gas circulates in a second heat exchanger (7), which acts as a radiation shield for the internal tank. This part is also used to cool actively the front radiation shield of the detector head.

Before leaving the vacuum vessel, the gas is circulating in the bottom heat exchanger (8) where it is warmed up via an integrated heater controlled by TC2 to 300 K in order not to create any ice on the exhaust pipe. The warm gas is stored in a small buffer container (14) at a pressure of 0.2 bar in order to supply the window defogging system and herewith avoiding condensation on the detector head entrance window by means of a gas flow. The OmegaCAM Cooling Controller has been developed to control the cooling system. Many of the cryostat external components (thermal sensors, valves, nitrogen tanks, transfer lines) are standardized ESO components.

The cooling system was designed such as to have a large hold time (42 hrs) and to be able to cool the CCD mosaic below the nominal operating temperature of -120 C.

The top heat exchanger is coupled by means of electrically isolated silver foils to cooling clamps which link directly to the bottom cooling fingers of the CCD mosaic table in the CCD detector head. This way the weight of the cooling system

(about 120 Kg) could be decoupled from the flexure of the mosaic table, vibration could be minimized and the position-angle dependent performance of conventional bath cryostat systems at Cassegrain focus could be overcome. As the cooling clamps can be opened and closed through the vacuum vessel, the cooling connections are easily separable before the detector head is mounted or dismounted (Figures 19 & 20).

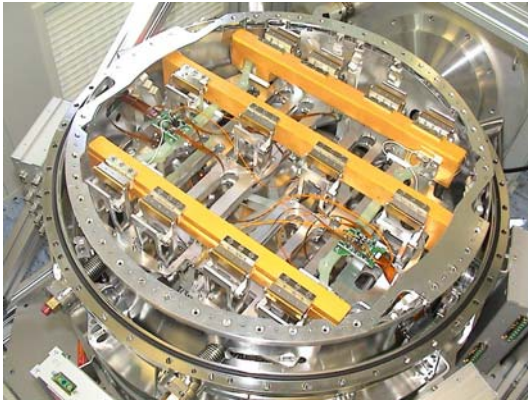


Figure 19: Cooling system top interface

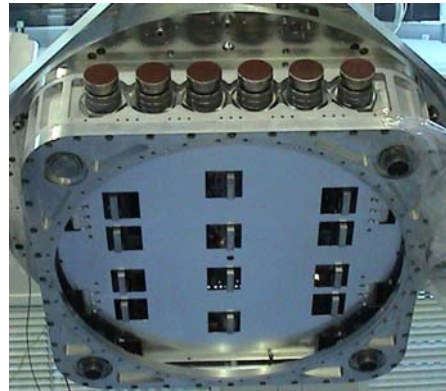


Figure 20: Detector head bottom interface

During laboratory operation, very good margins have been obtained to reach the necessary CCD operating temperature of -120 degrees C and a hold time of about 40 hrs. For the cryogenic and vacuum system control, the cooling system has integrated (heated) sensors for level sensing at top and bottom, a heatable charcoal sorption pump, and two fully redundant sets of temperature and vacuum sensors. Further details about the cooling system can be found in Lizon et al 2005.

7. TEMPERATURE CONTROL AND PULPO 2

Following the rough temperature control by the cooling controller imposed onto the cooling system, the CCD mosaic temperature is much finer regulated by ESO's new house keeping unit PULPO 2 (Geimer et al. 2005).

PULPO 2 (Figure 21) is a very compact unit (230x105x120mm) containing two Eurocard size (160x100mm) boards (Figure 22). The CPU-board contains an embedded PC running the PULPO 2 control software under Linux and provides power to the rest of the unit. The peripheral board contains all circuitry needed to fulfill the required housekeeping functions : 29 x four wire Pt100 inputs with freely programmable assignment to eight heater control circuits, amplifiers and 16 bit ADC, shutter interface, temperature and pressure alarm output, vacuum monitoring, and eight closed loop heater power outputs. The communication between the two boards follows the ISA bus standard.



Figure 21: Pulpo 2

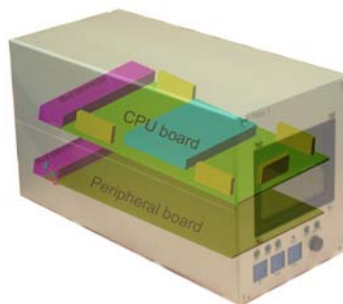


Figure 22: Pulpo 2 inside view



Figure 23: CCD head integrated dual multiplexer

In the case of OmegaCAM, Pulpo 2 interfaces to four multiplexer boards internal to the CCD head (Figure 23). With this arrangement the number of sensors could be increased up to 125, while the heat loss and cabling in the CCD head was minimized.

As diagnostics of the completely new construction of both the detector head and the cooling system (considering also all integrated electronics), about 100 temperature sensors with optional permanent logging were integrated into the cryostat at intermediate levels. They will again prove to be very useful for the checking of the cooling clamp interface after re-integration of detector head and cooling system in Chile.

Pt100 boards with standardized completely glue-free mechanical mounting interface have been developed for universal use. They interface by means of an interconnection kit in different lengths to the CCD head internal multiplexers.

The Pt100 sensors are monitored by PULPO2 which takes care of reading, logging and alarm signaling for all of them. Furthermore PULPO2 operates four independent PID heater control loops with freely programmable control sensor assignments. In full CCD mosaic operation a homogeneity of 4 K (pp) was achieved in the CCDs across the focal plane.

In addition PULPO2 interfaces via a specialized software shutter identifier to the OmegaCAM shutter, accurately times the exposure, and records open and close time as well as movement direction and an error signal for the encoder step counter.

8. THE CHALLENGES IN MULTIPLE CCD CONTROLLERS LINKED TO ONE SYSTEM

8.1 Coordination and synchronization of multiple CCD controllers

Three ESO standard FIERA CCD controllers are used to satisfy all operational needs. Two identical FIERA systems had to be assigned to one mosaic half. Each of them supports the maximum number of 4x4 video channels. Together with their associated UltraSparc control computers, they basically form two almost independent systems. But, because of the sharing of parallel and serial clocks, they had to be synchronized with high accuracy in soft- and hardware for wipe, integrate, and read functions of the mosaic CCDs. FIERA 1 operates as the master controller, which triggers the slave controller FIERA 2 and also communicates via PULPO2 with the shutter controller (Reif et al. 2005).

On FIERA 3 are defined software camera #1 for the two guider CCDs and software camera #2 for the two image analyzers. Its synchronization to the master controller is only needed for the shutter opening and the full-frame acquisition images of each auxiliary CCD. After the (automatic or interactive) selection of the guide stars and the setting of the respective readout windows and exposure times on the auxiliary CCDs, the operation sequence for a scientific exposure is as follows: Wipe both mosaic halves synchronously (FIERA 1 & 2), set to synchronized integration, open shutter. Start staggered continuous rapid readout loops with the two guiders (software camera #1 on FIERA 3). Ditto for the two image analyzer CCDs but somewhat longer exposure times (software camera #2 on FIERA 3). When camera #2 on FIERA 3 requires readout, operation of camera #1 is suspended. Both loops stop when the integration time on the mosaic is finished, the shutter is closed, and the subsequent synchronized readout of the two science mosaic halves takes place.

8.2 Synchronization of the mosaic halves and associated sensitivity

All CCDs in OmegaCAM are mechanically mounted onto the common mosaic table. Due to FIERA 1 & 2 being associated to one half each, the respective cables and their shields are all ending up on the detector head. Each FIERA unit has a power supply and a detector front end electronics box which can be mounted isolated or connected to the co-rotator structure and therefore also to the instrument ground. It is common knowledge to strictly obey synchronous clocking and to put digitization signals into quiet periods in a normal system. The sensitivity to non-synchronous events within this system is much higher due to the capacitive coupling of the CCDs on the mosaic plate and the respective grounding and shielding with multiple controllers operating identical functions with different clock generators. In a first step FIERA 1 & 2 were synchronized for their outside start pulse to an accuracy of +/- 20 nsecs. As a key element, all hard- and software of those two systems must be identical, except for some voltage settings for the respective CCDs.

The resulting CCD images proved to be the best indicator for subtle features resulting from this slight mis-synchronization: If the mosaic halves were not precisely synchronized, one mosaic half increased its bias level on all

channels for about 2 ADU's, whereas the other one decreased the bias level by the same amount. The sign of the bias change for the respective half was corresponding to the sign of the respective start pulse jitter. Therefore in the next step special care was taken on the software side to minimize the code processing the start pulse triggering the respective DSP, as well as on the hardware side to remove any potential start pulse jitter due to non deterministic hardware. With this solution a synchronization stable to 0ns was achieved which resulted in stable bias values of the CCDs. This proved to be necessary for all clocking operations of the two mosaic halves with an accuracy of 0 ns for the start of wipe, integration and readout operations. During the course of the rather long period of about 30 sec's where both halves are read synchronously - but with independent clock generators - no timing drift was observed.

8.3 Data chain and transfer performance over several computer levels

Following VLT control system standards, the remote control and the link to general facilities such as VLT data archive needed to be satisfied with the OmegaCAM detector system. Consequently the data stream has to pass several levels of computers and networking (Figure 24). The performance of data transmission, sorting and display is critical in view of a data volume of about 0.5 GByte per single frame. Several upgrades have been done recently in order to decrease the dead time between exposures.

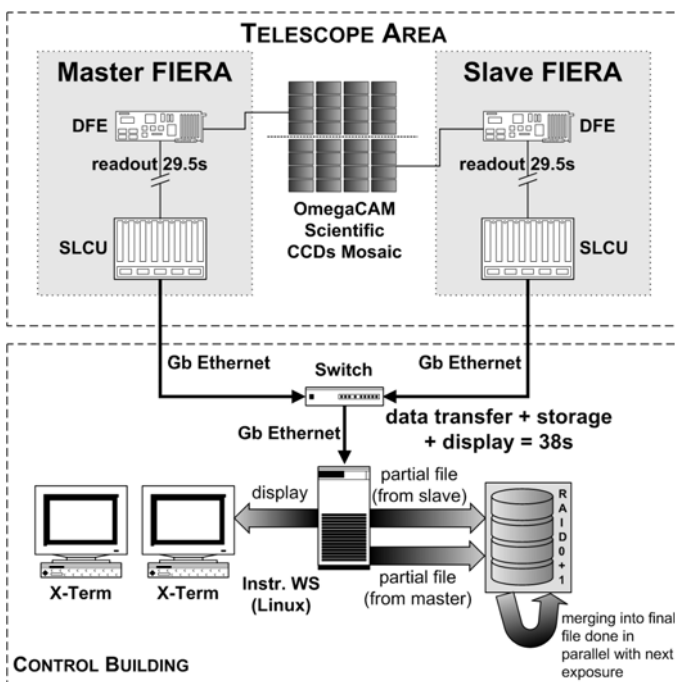


Figure 24: Remote control and data chain of FIERA 1 & 2

With respect to the original configuration the embedded computer of the FIERA controller (SLCU) has been upgraded to an Axi Motherboard Sun Blade 1500. Their connection to the instrument workstation is now based upon Gigabit Ethernet instead of ATM. The instrument workstation itself is now operating under Linux.

The data of the two half images are assembled, sent to the instrument workstation, combined, displayed, archived, and made available for automatic (pipeline) or interactive analysis. The full mosaic is read out in 29.5s with a read noise of $5e^-$. The overhead for file merging, storage and display adds 8.5s.

In case of a failure of one of the two controllers, the system can still be reconfigured in such a way that at least one mosaic half is read, whereas all other functions including the shutter operation can be maintained.

9. SAFETY & EMERGENCY FEATURES

During the daily nitrogen refilling operation, the cryostat cooling controller is responsible for a number of automatic, safety relevant actions, such as to trigger the interlock of the telescope motion and to open and close the relevant valves for the refilling process. Likewise PULPO2 takes preventive actions for the safety of the detector mosaic. E.g., it heats it up to a preset temperature in order to avoid uncontrolled warm-up and subsequent contamination in the case of operational errors or problems with the cooling or vacuum systems. In the case of vacuum loss, an on-board emergency pump with associated electromagnetic valve is activated. Both subsystems have user definable parameters in their

firmware for their respective alarms and emergency actions. They link to the Central Alarm System (CAS) which notifies maintenance personnel via wireless pagers. Loss of power and overheating of the FIERA controllers are signaled in the same way. Furthermore, the instrument control software can be configured for each of these parameters to issue a software warning on the instrument operator panel before the value of a hardware CAS alarm is triggered. Continuous logging of all essential parameters on the instrument workstation level permits trend monitoring and fault analysis.

10. SYSTEM QUALIFICATION AND RESULTS

Several independent qualification steps have been done in order to qualify the detector system for end use in Chile :

The CCDs were tested individually on the ESO test bench, the cryostat mechanics was qualified with the cooling system, the flexure of the mosaic table inside the head was tested with a dummy weight. The cleanliness and the vacuum and thermal properties of the cryostat after plasma cleaning were verified with the cold operation of mechanical sample CCDs. The cryostat electronics were tested offline with FIERA controllers. As a next step the cryostat was equipped with 16 mechanical samples and 16 engineering grades which enabled alternate operation and comparative qualification of FIERA 1 & 2. Upgrading the cryostat to the full science grade CCD configuration and all auxiliary CCDs enabled to test synchronization and full detector system performance.

At this point however the most important point was the unification of the OmegaCAM detector system with the OmegaCAM instrument, as to do complete long term system testing within the framework of the preliminary acceptance Europe. This was the first point where the overall system was available as one unit with completely integrated software and the overall quality of the system could be assessed.

After tests which e.g. proved that the filter exchange mechanism could be operated during the actual readout of the CCD mosaic without interference, the performance testing concentrated onto the testing of the auxiliary CCD loops with artificial stars and onto the CCD mosaic performance as a whole by means of automated CCD data pipeline software identical to the one used later on the telescope.

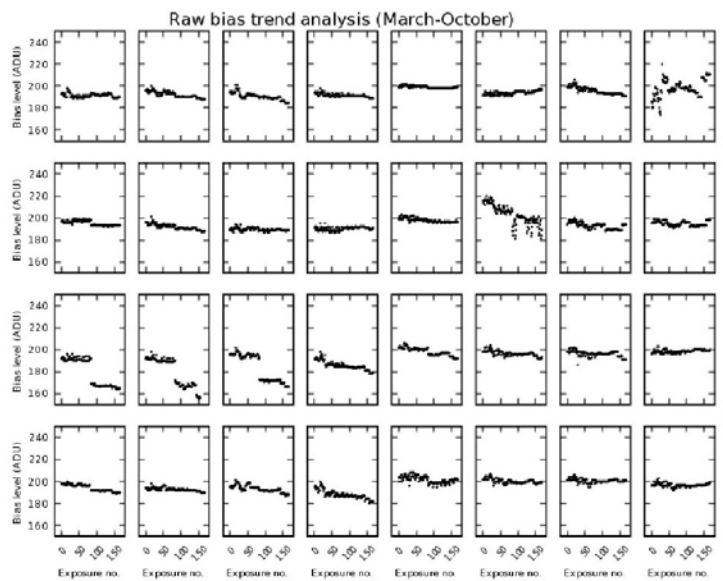


Figure 25: Bias statistics of individual mosaic CCDs in long system test

The problem to uniformly illuminate the whole field of the mosaic with suitable accuracy and at the same time to be able to project test patterns onto the mosaic to verify the image assembly software was solved by means of an inverse pin hole camera. A distant fiber coupled to a calibration lamp was used to illuminate the mosaic point source like, whereas the test patterns were directly inserted into the filter exchange mechanism, very close to the dewar entrance window.

Figure 25 shows one example of this long term automated testing where the detectors themselves and their peripheral parameters proved to be the best indicator for system deficiencies. Several factors were responsible for the uncorrected raw bias changes over eight months visible in the graphics. Amongst others these were the on-/offline time of the controllers, the cooling liquid temperature, as well as the swap of a video board.

Filling volume of internal nitrogen tank	40 l
Hold time of internal tank (continuous flow system)	42 hrs
Operating temperature of CCDs	-120 C
Number of used video channels	36
Readout speed	357 Kpix/sec
Readout noise of mosaic CCDs	< 5 e-
Variation of readout noise w.r.t. reference value	< 0.5 e-
Temperature variation across mosaic CCDs	< 4 C pp
Dark current of CCDs	< 2 e-/pix/h
Crosstalk between CCDs	5x10e-6
Number of bad pixels in complete mosaic	< 80000
Repeatability of measurement results in all detector domains of linearity and raw data	< 1 %
Flatness across cold mosaic w.r.t. mounting flange	< 40 μm pp
Minimum time between consecutive exposures	38 s
Total weight of cryostat	234 kg

Figure 26: Performance characteristics in a nutshell

Also the non-linearity of the photon transfer curve (Downing et al. these proceedings) could be reproduced.

Figure 26 shows the performance in a nutshell.

As a result of all tests so far the system works as expected with a stability and repeatability within 1 % over long term measurements.

As a side effect of all this testing many fault situations could be analyzed and the related alarms, system reliability, and firmware of subsystems improved.

11. SYSTEM STATUS

After long term system tests together with the instrument during 2005, the detector system is currently undergoing last tests on a moving stand as to verify the thermal and electrical behavior at different operating angles. The installation date in Chile is dependent on the completion of the VST telescope.

12. ACKNOWLEDGEMENTS

The OmegaCAM detector system was designed and built by the ESO Optical Detector Team with major contributions from other ESO departments, largely financed by the OmegaCAM consortium.

OmegaCAM is funded by grants from the Dutch Organization for Research in Astronomy (NOVA), the German Federal Ministry of Education, Science, Research and Technology (grants 05 AV9MG1/7, AV9WM2/5, 05 AV2MGA/6 and 05 AV2WM1/2), and the Italian Consorzio Nazionale per l'Astronomia e l'Astrofisica (CNAO) and Istituto Nazionale di Astrofisica (INAF), in addition to manpower and materials provided by the partner institutes (ESO, Kapteyn Institute Groningen, Leiden Observatory, University Observatories of Munich, Göttingen and Bonn as well as Padua and Naples Observatories).

REFERENCES

- Baade, D. et al., 2004, Kluwer, ASSL, vol. 300, p. 197
Beletic, J. et al., 1998, Kluwer, ASSL, vol. 228, p. 103
Cappacioli, M. et al., 2005, The ESO Messenger, No. 120, p. 10
Christen, F. et al., 2004, Kluwer, ASSL, vol. 300, p. 485
Christen, F. et al., 2006, Springer, ASSL, vol. 336, p. 537, 543
Deiries, S. et al., 2006, Springer, ASSL, vol. 336, p. 129
Downing, M. et al., these proceedings
Geimer, C. et al., 2006, Springer, ASSL, vol. 336, p. 589
Kuijken, K. et al., 2004, Proc. SPIE, vol. 5492, p. 484
Lizon, J.L. et al., 2006, Springer, ASSL, vol. 336, p. 143
Reif, K. et al., 2006, Springer, ASSL, vol. 336, p. 147
VLT Control System Specifications VLT-SPE-ESO-17000-1088